Experimental Thermal and Fluid Science 52 (2014) 308–317

Contents lists available at ScienceDirect

Experimental Thermal and Fluid Science

journal homepage: www.elsevier.com/locate/etfs

Experimental study on defrosting mechanism of intermittent ultrasonic resonance for a finned-tube evaporator

Haihui Tan [a], Tangfei Tao [a,b], Guanghua Xu [a,c,*], Sicong Zhang [a], Dingyuan Wang [a], Xiangui Luo [a]

[a] School of Mechanical Engineering, Xi'an Jiaotong University, Xi'an 710049, China
[b] Key Laboratory of Education Ministry for Modern Design and Rotor-Bearing System, Xi'an 710049, China
[c] State Key Laboratory for Manufacturing Systems Engineering, Xi'an 710049, China

ARTICLE INFO

Article history:
Received 29 January 2013
Received in revised form 29 September 2013
Accepted 14 October 2013
Available online 23 October 2013

Keywords:
Ultrasonic resonance defrosting
Defrosting mechanism
Forced vibration
Excitation frequency
Natural frequency

ABSTRACT

This paper proposed a new defrosting method based on ultrasonic resonance mechanism, to solve the problem of the unknown mechanism of ultrasonic defrosting for a finned-tube evaporator. Dynamic microscopic process of frost crystals formation and growth under the natural frost condition was first investigated. According to the growth characteristics of the frost crystals, the natural frequencies of frost crystals with different height were calculated in COMSOL software. An ultrasonic transducer of 28 kHz/60 W was adopted as an executor to excite the evaporator, then ultrasonic defrosting experiments and laser vibrometer experiments were carried out under the excitation of the ultrasonic transducer. Finally, experiment of ultrasonic resonance based on intermittent operational was studied to optimize ultrasonic loading method. It was found that the height of the frost crystals were about 0.5 mm after growing for 4 min, the average natural frequency of the frost crystals were about 27.95 kHz, the evaporator and frost crystals on the fin surface were forced vibration at the frequency of 28.2 kHz, which was the actual working frequency of the ultrasonic transducer detected in laser vibrometer experiment, and most frost crystals with certain shape and size were immediately broken up when the ultrasonic vibration applied. The main mechanism of ultrasonic defrosting was the resonance effect of natural frequency of frost crystals and excitation frequency, and the optimal working mode of ultrasonic resonance defrosting was intermittent 4 min, vibration 1 min. The experiment's results also showed that ultrasonic shear stress and acceleration effect of ultrasonic also had defrosting performance, but they were not the main mechanism for ultrasonic defrosting.

1. Introduction

Frost formation on the surface of a finned-tube evaporator is often encountered under a low ambient temperature in winter. The thermal resistance increases and air channels blocks the heat-exchanger due to frost deposition, which the heat-exchange efficiency decreased drastically. Even the refrigeration system is shutdown due to the impact of refrigerant droplets against compressor blades. Therefore, developing an effective method to prevent evaporator frosting is crucial in the field of refrigeration and air conditioning.

In the past few years, there are many studies concerning the anti-frost and defrosting technology which uses external fields. For example, Liu and Tang [1] presented a dynamic simulation model of an air-source heat pump during hot-gas defrosting. They set up a nominal 0.88 kW capacity residential air-to-air heat pump during the defrosting, the simulation results are consistent with the experiment data. It also shows that the model is suitable for the simulation of performance characteristics of defrosting cycles. Cho et al. [2] measured the performance of an on–off cycle and hot-gas bypass defrosting of three showcase refrigeration evaporators. The study result showed that the optimum electronic expansion valve (EEV) opening was 75% of the full openings during the hot-gas bypass defrosting. The hot bypass defrosting cycles showed advantages in achieving the appropriate refrigerating capacity and maintaining constant storage temperature compared to the on–off cycling, although it had a relatively higher compressor power. Hoffenbecker et al. [3] proposed a transient model to predict the heat and mass transfer effects for an air-cooling evaporator during a hot gas defrosting cycle. Parametric analysis results showed that an optimum hot gas temperature is a function of both the accumulated mass and density of frost on the evaporator, and the model predicted that the mass of moisture re-evaporated back to the space increased with decreasing hot gas temperature. Qu et al. [4] experimentally studied a novel reverse-defrosting method which used phase change material (PCM) to storage the

* Corresponding author. Address: Mailbox 2314#, School of Mechanical Engineering, Xi'an Jiaotong University, Xi'an, Shaanxi 710049, China. Tel./fax: +86 29 82663707 80.
E-mail addresses: xy_thh@163.com (H. Tan), taotangfei@mail.xjtu.edu.cn (T. Tao), xugh@mail.xjtu.edu.cn (G. Xu).

0894-1777/$ - see front matter © 2013 Elsevier Inc. All rights reserved.
http://dx.doi.org/10.1016/j.expthermflusci.2013.10.006

Nomenclature

BLT	bolt-clamped Langevin-type transducer
s	second
ρ	material density
n	=1, 2 layer number
t	time
ψ	equivoluminal strain
c_L	longitudinal wave velocity
k_L	$=\omega/c_L$, longitudinal wave number
θ_L	angle of longitudinal wave propagation direction and normal direction
C_1, C_2, C_3, C_4	arbitrary constants
nu	Poisson ratio
E	elastic modulus
W×L×H	width(mm) × length(mm) × height(mm)
μ	=G, shearing modulus
λ	lame constants
∇^2	$=\partial^2/\partial x_1^2+\partial^2/\partial x_3^2$, differential operators
ϕ	dilatation strain
ω	angular frequency
c_T	shear wave velocity
k_T	$=\omega/c_T$, shear wave number
θ_T	angle of shear wave propagation direction and normal direction
a	acceleration
T_{zx}, T_{zy}	shear stress in x_1x_2 plane

thermal energy. Compared to standard defrosting condition, the PCM-based reverse-cycle defrosting method could shorter the defrosting time with higher suction pressure, the defrosting COP was increased and did not degrade the quality of space heating during heating operation, and indoor thermal comfort was improved for occupants during defrosting and heating resumption process. A transient simulation model of an air-coil evaporator to predict and evaluate the performance of the hot-gas defrosting process was developed by Dopazo et al. [5]. A finite difference approach was used to solve the model equations, the defrosting time and energy supply were increased as the refrigerant mass flow rate decreases or the inlet refrigerant temperature increase. The percentage of energy used to warm and melt the frost increases as the refrigerant mass flow rate increases (from 40.36% to 43.52%), and the minimum value of the percentage (32.2%) was found around 294 K.

As concluded in the research results above, hot gas and reverse cycle defrosting can remove frost effectively and inhibit frost deposition on the evaporator. With the common disadvantage of seriously penalizing the overall heat pump or air-conditioner efficiency, for they not only release cryogenic energy to the room, but also use energy during defrosting. Before defrosting, the heat pump or air-conditioner operated in low efficiency because of deposition frost which increases the thermal resistance and decreases air mass flow.

Relative to the hot gas defrosting, numerous researchers focused on the frost formation subjected to the influence of electric field. Munakata et al. [6] have studied the effect of electric fields on frosting phenomenon in 1998. They found a critical value, which the frosting rate was gradually decreased by increasing the electric field strength up to this certain value. After this critical value, the frosting rate was increased by increasing the field strength. Wang et al. [7] found that with the presence of electro hydrodynamics (EHD), the frost crystal was pulled up towards the electrode and the structure was relatively skinny and fragile to easily break up and fall off due to the influence of gravity. The speed of the frost growth and the break-off frequency under negative polarity was roughly 30–50% higher than those with the positive polarity. This phenomenon is related to the opposite direction of the dielectrophoretic force and the electrostrictive force at a positive polarity, whereas the direction of the dielectrophoretic force and the electrostrictive force are the same at a negative polarity. Tudor and Ohadi [8] firstly studied the effect of stationary and sweeping frequency AC electric fields on frost crystals growth and frost control/removal. They used electric field with sweeping frequencies (from 370 Hz to 7.5 kHz) at an applied voltage of 14.5 kV, the 46% reduction of frost was obtained, and most crystals were pulled by the applied oscillating electric force in the first 10–60 s. Zhang et al. [9] investigated the influences of direct current (DC) electric fields on the initial form of the frost crystal on a cold vertical plate. The experimental results showed that at the initial stages of the frost formation that the stronger the electric field, the smaller the water drops formed on the cold plate. They also found the frost mass increases with the electric field intensity. Joppolo et al. [10] experimentally studied the influence of a DC electric fields on the performance of a finned-tube evaporator under frosting condition and found that the electric field can reduce the frost mass and air-side pressure drop. To conclude, the use of the EHD technique could provide beneficial results for applications where frost insulating effect and air flow blocking effects were important and detrimental for the system working conditions. Generally speaking, the use of applied electric field could not remove frost completely, but it could delay or suppress frost deposition under certain condition. Therefore, exploration of a long-term effective frost suppression technology and application of it into practice was very important, which could achieve the purpose of energy saving and system performance optimization for the foundation of commercial application.

In addition to the above frost suppression technology, ultrasonic frost suppression technology was firstly studied by Adachi [11,12] in 1998. They used ultrasonic flexural vibration to excite a rectangular duralumin plate (20 mm × 92.6 mm) in almost 100% relative humidity at 2 °C. The defrosting experimental showed that the frost was decreased by almost 60% with the frequency of approximately 37 kHz and amplitude of 3.1 μm. The authors attributed this effect to the movement of small frost crystal nuclei which cannot stay on the plate to grow when the vibration amplitude is high. Yan et al. [13] experimentally studied the ultrasonic defrosting on a heat-exchange with a 40 m^2 refrigeration fan. The results proved that ultrasonic defrosting technology is feasible for refrigeration fan, and the transverse wave defrosting effect is better than vertical wave. Li et al. [14] investigated the initial frost nucleation, structure and thickness on a plate surface with and without 20 kHz noncontact ultrasound wave for 10 min. The experimental results showed that the sizes of deposited freezing droplets on the cold surface with the effect of ultrasound are much smaller than that without ultrasound and the shape is relatively inerratic. The ultrasound has a strong ability to restrain the initial frost nucleation and frost growth process. However, the impacted area of noncontact ultrasonic was small, the noncontact ultrasound cannot effective remove when the whole evaporator had frosted. Wang et al. [15] used dynamic microscopic process to investigate the frost formation and growth with and without ultrasonic vibration. They concluded that the mechanism of ultrasonic frost suppression was mainly attribute to the mechanical vibration effect, but the reason why low-frequency mechanical vibration have not frost suppression effect was not explained yet.

Understanding the defrosting mechanism of ultrasonic high frequency vibration is the prerequisite to realize the optimal ultrasonic working mode and energy saving. The contribution of this paper is explicated the mechanism of ultrasonic defrosting to optimize the ultrasonic defrosting effect. The evaporator was placed in a chamber to detect the characteristics of frost crystal formation and growth through dynamic microscopic process, according to the growth laws of frost crystal, the natural frequency of frost crystals with different height was calculated. The vibration of the evaporator under ultrasonic excitation was detected by the use of laser vibrometer under ultrasonic excitation, and the vibration frequency of the evaporator was recorded. The optimal intervention mechanisms, intermittent time and working time of ultrasonic high frequency vibration were confirmed based on the natural frequency of the frost crystals and the vibration frequency of the evaporator.

2. Experimental setup

Fig. 1 shows that the whole experimental apparatus which consists of a constant temperature chamber, a set of commercial vehicle air-conditioning systems, ultrasonic vibration system, microscopic image system and data acquisition system. The temperature (between −20 °C and 120 °C) and relative humidity (between 40% and 95%) of the chamber is kept constant to offer a condition with stable temperature and humidity. The compressor and the condenser are put outside the chamber, the evaporator is placed inside the chamber, the condenser and the evaporator connected through a braze pipe which passed through a hole on the left side of the chamber.

The air-conditioning system uses a compressor as a cold source, the capacity of the compressor is 100 W, the COP is 1.4, refrigerant uses R600a, a finned-tube evaporator used to extract the heat from the chamber and frost deposit on its surface. The size of the evaporator is 270 mm × 300 mm × 12 mm ($W \times L \times H$), where W represents the transverse length of the evaporator, L represents the longitudinal length of the evaporator, H represents the depth of the evaporator. W, L, and H are the abbreviation of width, length and height, respectively. The aluminum fins surfaces are covered with hydrophilic coatings whose contacts angle of the water drop is 37.7°, the frontal width of the fin is 12.08 mm, frontal height of the fin is 290 mm, depth of the fin is 0.097 mm, and the interval between each two fins is about 1.55 mm. The inside diameter of the pipe is about 5.9 mm, longitudinal pitch of the pipe is 21 mm, and the evaporator is single layer structure. In order to understand the specific parameters of the evaporator more intuitively, the specification of the evaporator was shown in Fig. 2.

The microscopic image system is comprised of a microscope and a micro camera. The microscope can be adjusted continuously to change its magnification. The micro camera (a CMOS camera TCAM3) is connected to the microscope with a camera lens. The amplified frost images captured by the camera are transferred to a PC and processed through the application software, the dynamic images can be displayed on the computer and saved to the disk. A LED cold light source is used for illumination to avoid melting the frost during the experiment. Some tiny characteristics of frost crystals observed by the microscopic image system could be clearly seen during the frosting experiment for understanding the frosting process and characteristics of frost crystals. Therefore, the effective measurement and observation can be ensured by using a microscopic image system.

The ultrasonic vibration system is comprised of a digital ultrasonic power supply and a BLT transducer which the resonance frequency is 28.2 kHz, the maximum power is 50 W. The frequency of ultrasonic power can be set and adjusted, the maximum output power is 300 W, and the frequency can be set from 15 kHz to 60 kHz. The ultrasonic power supply also has frequency auto tracking function, the step frequency can be distinguished by 0.01 Hz.

3. Experimental results and discussion

3.1. Growth characteristics of frost crystal

Experiments of frost deposition on the fin surface are investigated by using microscopic visualization measurement, the video and the pictures are continuously recorded after the compressor start to work. Fig. 3 shown that the frost deposit process under the ambient temperature (AT) is 9.8 °C, the relative humidity (RH) is 89%. Small water droplets firstly appeared on the fin surface when the compressor worked for 2 min, the temperature of the fin surface dropped to about −2 °C. Subsequently, small water droplets are continuously precipitated and a thin water film is formed with the lapse of time. With temperature around the evaporator decreasing continuously, the latent heat of water film is released and frozen to form an adhesion ice layer on the fin surface. When the compressor has worked for 6 min, the temperature field near the evaporator tends to stabilize. Then the water vapor in the air directly begin to condense and form a frost crystal on the adhesion ice layer, these initial frost crystals grow independently along the vertical direction of the fin surface. The frost crystals formed in the early stage were presented slender feather or needle feature with lower strength and relatively sparse. The frost crystals form an overlapping pattern, and the structural strength is increased after the initial frost crystals growing to a certain extent.

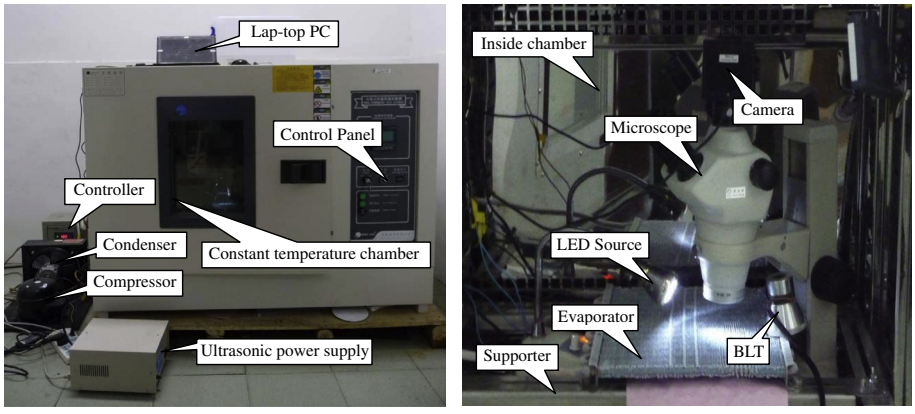

(a) Experimental apparatus outside the chamber (b) Experimental apparatus inside the chamber

Fig. 1. The whole experimental apparatus for frost suppression tests.

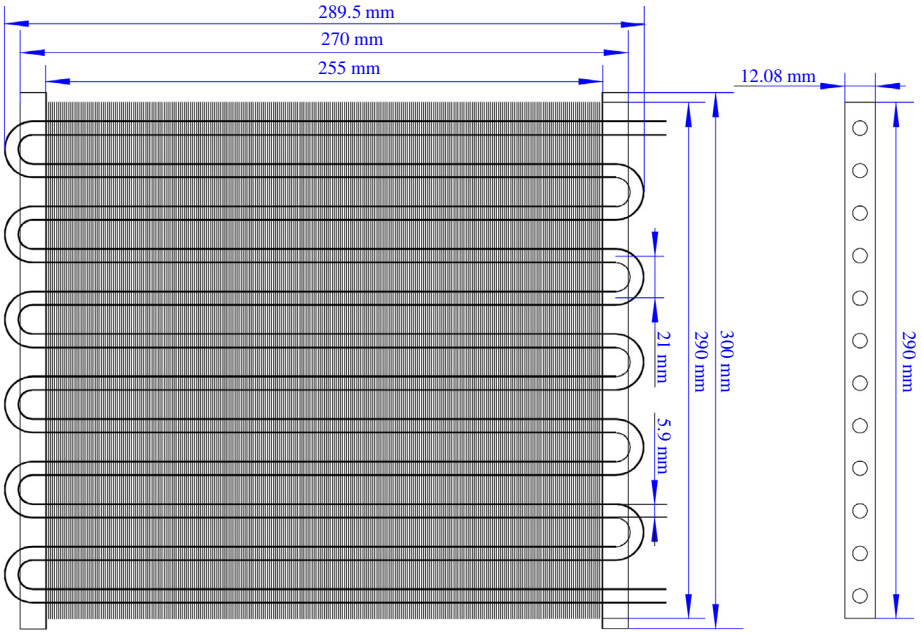

Fig. 2. The specific parameters of the evaporator.

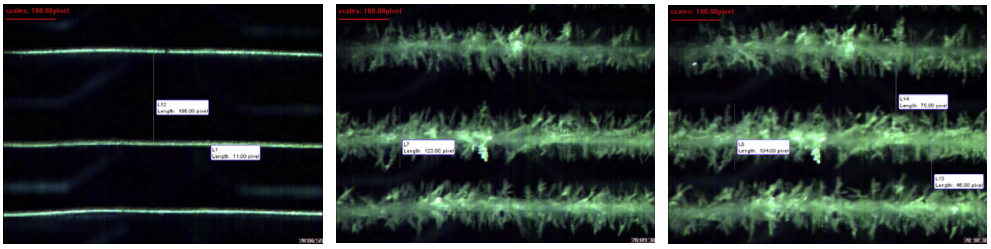

(a) compressor started to work (b) compressor worked for 180 s (c) compressor worked for 240 s

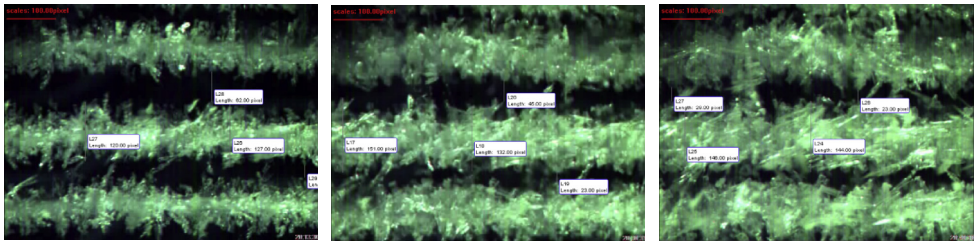

(d) compressor worked for 420 s (e) compressor worked for 1441 s (f) compressor worked for 2040 s

Fig. 3. Microscopic images of frost crystal growing process (11 pixels = 0.0917 mm).

Fig. 4 shown the trend of fin surface temperature varies with time. In the surface of the evaporator, the adhesion ice layer increased the thermal resistance of thermal conductivity, which made the heat exchange of the refrigerant insufficient. Although the initial environmental temperature and humidity were different, the surface temperatures of the evaporator were similarly after they reached steady state, and the trend graph of surface temperature varies with time was also similarly based on the experimental results. So the trend of cooling surface temperature and the stable temperature under the condition of AT = 9.8 °C and RH = 89% could be used as a general trend for our different experimental environment conditions.

When the compressor works for 2490 s, the intervals between any two fins is blocked by frost. The measurement system is calibrated by using a standard circle with its diameter (the maximum is 1 mm, the minimum is 0.1 mm), with the help of measuring module, the height of frost crystals and intervals between any two fins at different times are measured. In order to obtain the approximately exact value of the frost layer thickness, the multi-points are measured and the average value is obtained to gain the accurate value of the frost layer thickness.

As shown in Fig. 5, the double sides frost thickness on the fin surface is increased with the time elapse. Frost grows fast during the first 5 min in the natural frost condition, then the frosting speed slows down. There are two main reasons for this phenomenon: (1) The thermal resistance increases due to the adhesion ice layer, the amount of the heat exchange between fins and air is decreased. (2) The air pressure is increased because the air channels are blocked by frost, the air flow is decreased which resulted in the reduction of the heat exchange. The black curve in Fig. 3 is the frost thickness after the experiment condition (AT of 18 °C, RH of 84%), amount of water droplets were on the fin surface with the faster

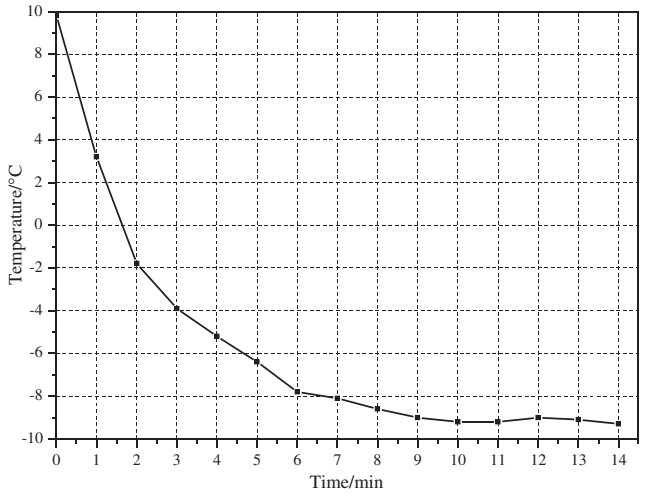

Fig. 4. The curve of fin surface temperature varies with time.

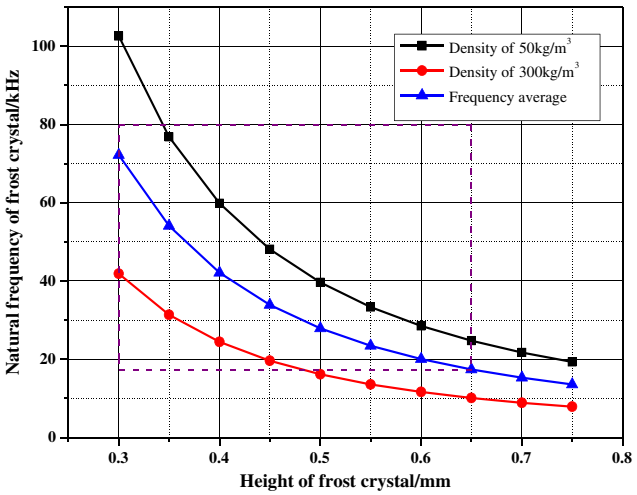

Fig. 6. The natural frequencies curve of frost crystals at initial stage.

frosting speed than the other two conditions. The experiment condition correspond to the purple curve (AT of 6 °C, RH of 85%) is in the fourth day after the black curve condition, the fin surface is clear in the start of the experiment. Partial pressure of water vapor contained in the air is low because of the lower ambient temperature, so less liquid water droplets is precipitated as the ambient temperature decrease. The effect of measurement error and measurement point are not taken into account, therefore, the defrosting time interval should be less than 6 min based on frost growth characteristics.

According to the frost crystals growing characteristics, the frost crystals are simplified to a truncated cone with one twelfth of the ratio of diameter to height and 1° of draft angle based on the frost crystals growing characteristics. The frost crystal physical model of 0.75 mm height is established in COMSOL soft. The height of 0.70 mm, 0.65 mm, 0.60 mm, 0.55 mm, 0.50 mm, 0.45 mm, 0.40 mm, 0.35 mm, and 0.3 mm are created with the unchanged diameter. After that, the natural frequency of each model is calculated, and the density of the frost crystal is chosen according to reference [16], the Young modulus and Poisson ratio are referred to rime ice (E = 5.3E7, nu = 0.3).

The natural frequencies of the frost crystals at initial frosting stage are shown in Fig. 6, the height of independent frost crystals are generally less than 0.7 mm. If the height of frost crystal is larger than 0.7 mm, they present an overlapping growing pattern, the length of frost crystals less than 0.3 mm are not considered here. From the frequency distribution diagram, the natural frequencies of different heights frost crystals range from 14.7 kHz to 72.2 kHz, and the natural frequency of frost crystal decreases with the growth of the frost crystal. Therefore, it is possible to conclude that the early frost crystals and the external ultrasonic low frequency vibration excitation has resonance characteristic to some extent. The amplitude of frost crystals will sharply increase according to the resonance theory, and finally break up.

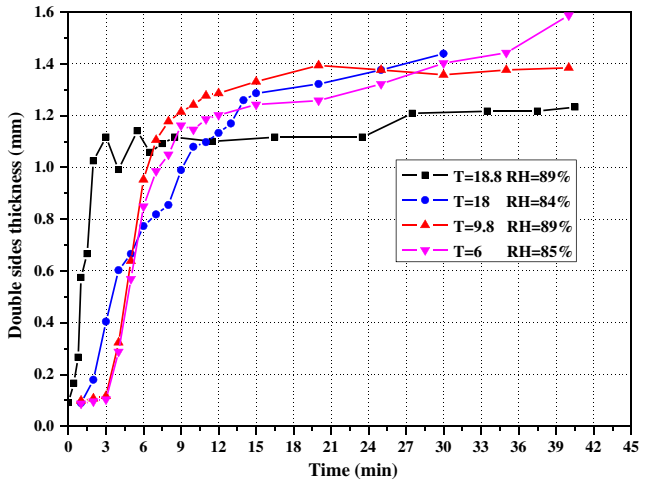

Fig. 5. The curve of double sides frost thickness varies with time.

3.2. Proposal of intermittent ultrasonic resonance defrosting method

In Figs. 5 and 6, the natural frequency of frost crystal is close to the external ultrasonic excitation frequency after frost crystal growing for a certain time. According to this feature, a new ultrasonic resonance high-efficiency defrosting method based on intermittent operation mechanism is presented in this paper. In order to optimize ultrasonic vibration defrosting effect, the resonance effect of ultrasonic vibration and frost crystals is used to realize the high efficient defrosting. During the experiments, a small refrigeration compressor as cold source for the evaporator, a constant temperature and humidity chamber is used to offer a controllable condition with stable temperature and humidity. Choosing natural frosting condition as a standard, the defrosting effects are investigated in five types working mode of ultrasonic transducer (natural frosting condition, intermitted 4 min and vibrated 1 min, intermitted 5 min and vibrated 1 min, intermitted 8 min and vibrated 1 min, continuous vibration) under the ambient temperature of the chamber is 6 °C, and RT is 85% in natural convection.

Fig. 7 shows the microscopic frosting figure at different time in natural frost condition, the frosting speed is quick at first 10 min in the low temperature and high humidity, then slowing down. Frost crystals with similar shape are formed on both sides of the fin. The growth direction characteristics of the frost crystals are showing one-dimensional which is perpendicular to the fin surface. When the compressor runs continuously for 40 min, the fin gaps are almost blocked with frost.

Throughout the whole defrosting process as is shown in Fig. 8, the frost crystals on both sides of the fin are cracked under ultrasonic resonance vibration and falling off under gravity. The frost layers on both side of the fin are increased slowly and the density of the frost layer is lower with the thickness increasing, but the ultrasonic resonance vibration defrosting effect is still significant

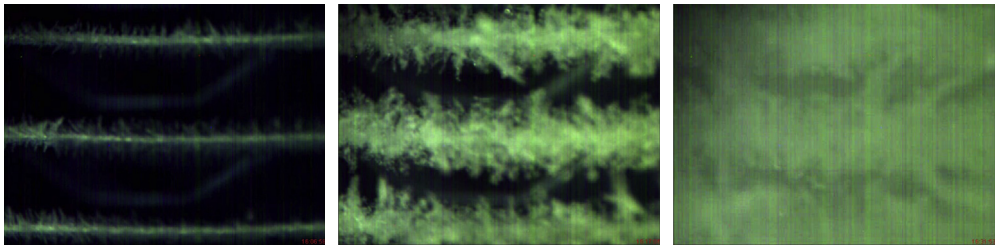

(a) frosting 5 min (b) frosting 15 min (c) frosting 30 min

Fig. 7. Microscopic frosting images in natural frost condition.

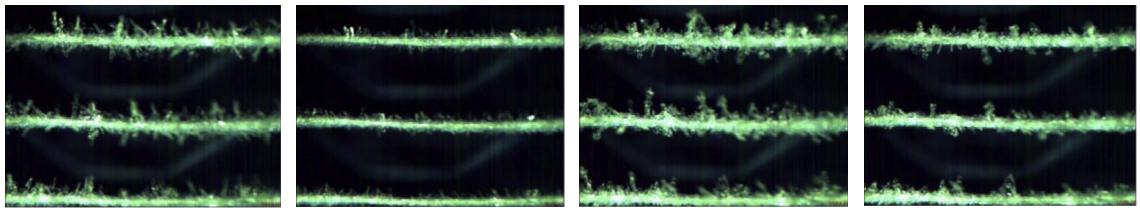

(a) 15min/16min (b) 20min/21min

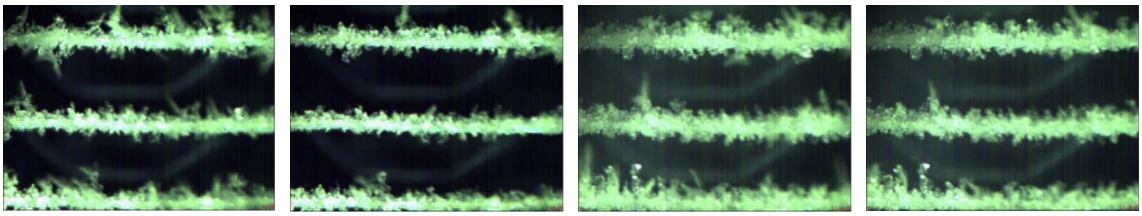

(c) 40min/41min (d) 90min/91min

Fig. 8. Microscopic frosting images under intermitted 4 min, vibrated 1 min.

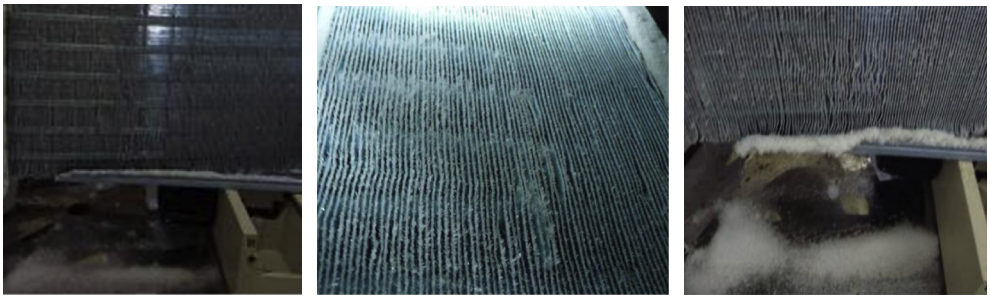

(a) removed frost at 56 min (b) frost on the evaporator surface at 90 min (c) removed frost at 141 min

Fig. 9. Macroscopic images of removed frost on the front side of the evaporator.

if the intermittent time is proper. When the experiment is carried out to 90 min, the entire surface of the evaporator with only small amount of frost, the fin gaps are not blocked with frost. This indicates that the intermittent ultrasonic defrosting is more effective than continuous ultrasonic defrosting.

Fig. 9 shows the condition of defrosting effect on the front side of the evaporator after the compressor working for 141 min. From the macroscopic images, some conclusion can be drawn:

(1) Under the influence of intermittent ultrasonic vibration, there is only basic thin ice layer on the fins surface, and there is no frost apparently deposited on the fins, the fin gap distances are nearly kept the initial state, the fin gaps are not blocked.
(2) Under the evaporator, there are some frost piles that forms with the fractured frost crystals and branches, even frost piles that accumulates on the fins.
(3) The high frequency ultrasonic vibration breaks the frost crystal on the fins and fall off with the gravity, so that makes the fin gaps are not blocked after a long experiment time.

Figs. 10 and 11 show the microscopic frosting images under different working modes. The mode of intermitted 5 min then vibrated 1 min can broken the frost crystals effectively. Frost layer thickness is about one-third of the fin pitch after the compressor worked 30 min, the frost layer thickness not increased, but there are some frost balls on the fins with time lapse, almost all the fin gaps are blocked after the compressor working for 60 min. Frost

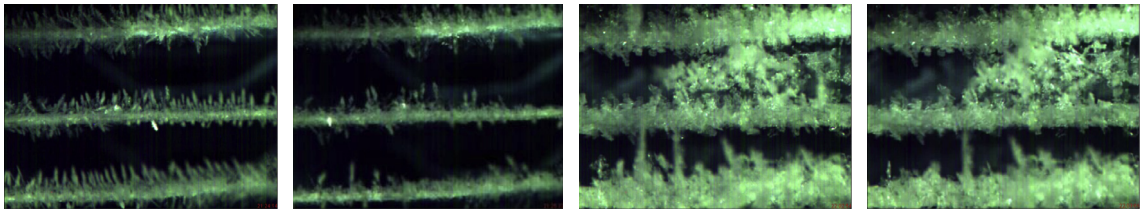

(a) 5 mim/6 min (b) 45 min/46 min

Fig. 10. Microscopic frosting images under intermitted 5 min, vibrated 1 min.

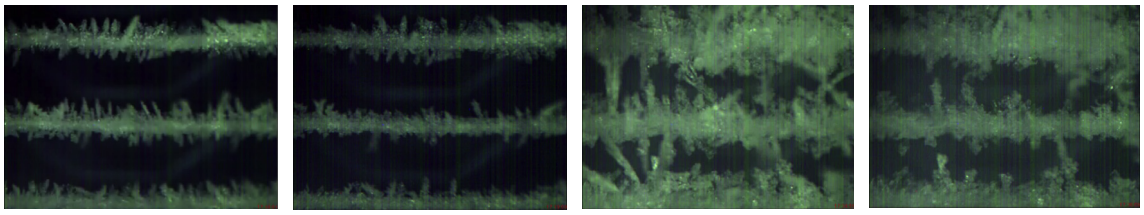

(a) 8 mim/9 min (b) 26 min/27 min

Fig. 11. Microscopic frosting images under intermitted 8 min, vibrated 1 min.

crystals grow along two-dimensional direction from the 6th min in mode of intermitted 8 min then vibrated 1 min. The natural frequency of the frost crystals is lower than 10 kHz due to the extremes length of the interval time, which is difficult to resonance with excitation frequency. The ultrasonic defrosting effect is not significantly, most of the fins are blocked with frost after the compressor operated 30 min.

In Fig. 12, the effect of ultrasonic defrosting is sound and effective at early stage of frosting process, and the optimal ultrasonic working time interval should be 3–4 min, for each vibration, a short working time (10–30 s) is enough. The mechanism of frost removal can be attributed to resonance effect between the natural frequencies of frost crystals and the ultrasonic vibration frequency, when the natural frequency of frost crystals is equal or similar to ultrasonic vibration frequency, frost crystals can be easily removed. Natural frequency is decreasing with the frost crystals growth in the interval time, when the frost crystals grow for 3–4 min according to Fig. 4, the natural frequency of the frost crystals are range from 22 kHz to 30 kHz, while the ultrasonic working frequency is 28.4 kHz to 28.6 kHz, the author believe that the ultrasonic excitation frequency has a resonance effect with natural frequency of frost crystals. In conclusion, digital ultrasonic power supply with the frequency auto tracking function is suitable for a better effect of ultrasonic frost removal.

With the difference of the size, shape and growing velocity, frost crystals form a series of natural frequencies. Not all frost crystals are removed by using ultrasonic transducer with a constant frequency at one time. Therefore, it is necessary to analysis the ultrasonic intervention time, intervention cycle and vibration time.

(1) Ultrasonic vibration should be intervene at initial frosting stage which frost crystals are growth independent in one-dimensional direction, the natural frequency is matched the resonance frequency of the ultrasonic vibration which can be easily fractured in 5 s as soon as the transducer worked, the remnant frost crystals are partly and gradually removed in the later vibration stage (5–30 s). Therefore, the intermittent time should not exceed 5 min, if the intermittent time is too long, the natural frequency of the frost crystal is decreased below to 10 kHz, which is out off the frequency band of the ultrasonic digital power supply, that means the resonance effect of ultrasonic vibration and frost crystals are not occurring.

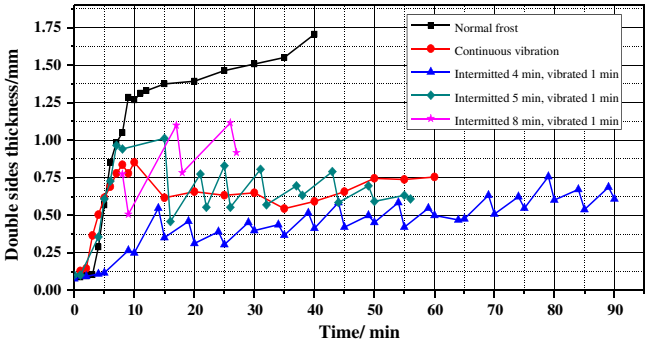

Fig. 12. Frost thickness on the both sides of the fin under different intermittent time.

(2) The intervention cycle of ultrasonic vibration depends on growing speed of frost crystals and frosting condition. If ambient temperature and ambient relative humidity are high, while the evaporator surface temperature is low, the intermittent time should be setting relatively shorter. Otherwise, the intermittent time should be setting relatively longer. Ultrasonic vibration with different time intervals has different impacts on the experiment temperature and work frequency of ultrasonic transducer, a proper time interval should be adjusted to ensure the normal working of the ultrasonic system. Based on a large number of frosting experiment data, the ultrasonic transducer is fuzzy controlled according to temperature data and relative humidity data which is detected by temperature data and humidity data logging devices. In this paper, the recommended intervention cycle is 5 min, which intermitted time is 4 min, vibrated time is 1 min.

(3) Through the previous defrosting experiment, the author has discovered that the frost crystals on both sides of the fin are broken up and fell off after the ultrasonic transducer

working for 5 s. Subsequently, the frost crystals are growth and fell off constantly, most of the frost crystals on the fins have been removed when the ultrasonic transducer working for 30 s. Therefore, the authors suggested that the ultrasonic vibration time should set to 5–30 s.

3.3. Analysis of intermittent ultrasonic resonance defrosting mechanism

3.3.1. Experimental study of ultrasonic resonance defrosting

In the aim to verify this hypothesis of ultrasonic resonance defrosting, an ultrasonic defrosting experiment was carried out in Nov. 26 2009 in free convection, the temperature around the evaporator was about 10 °C and 85% RH. During the defrosting experiment, the minimum temperature on the fin surface was about −9 °C. As shown in Fig. 1, the evaporator was placed inside the chamber. The compressor run continuously from the beginning, the ultrasonic transducer began to work after the compressor started with the work mode that intermitted 4 min and then vibrated 1 min. Six cycles were included in the 1 min, and the mode of each cycle was broken 5 s and then vibrated 5 s, the entire process of frosting under the influence of ultrasonic high frequency vibration was 153 min in all.

An interested phenomenon is found in the microscopic visualization study of entire ultrasonic high frequency vibration defrosting process. Frost crystals with certain size and shape are suddenly broken up when the ultrasonic transducer is working, then remaining frost crystals fall off individually under the effect of ultrasonic high frequency vibration. The microscopic images of frost crystals under ultrasonic high frequency vibration for 1 min are shown in Fig. 13. Most of the frost crystals are broken off in the first 5 s when the ultrasonic high frequency vibration is applied, and the broken frost crystals are similar in some extent. From 5 s to 60 s under the ultrasonic forced vibration, frost crystals are cracked and fall off gradually. After the ultrasonic transducer vibration for 30 s, there are a few frost crystals left on both sides of the fin. Finally, there is only the adhesion ice layer on the fin surface. On the basis of the experiment phenomenon, the resonance characteristic of broken frost crystal and ultrasonic high frequency vibration can be confirmed in some extent. In other words, the nature frequency of the frost crystals with certain shape and the ultrasonic excitation frequency are same or similar, the frost crystals are easily to remove.

3.3.2. Experimental study of laser vibrometer

In the aim to further verification this hypothesis of ultrasonic resonance defrosting, the vibration of the evaporator under ultrasonic excitation is measured by using a high-precision PSV-400-3D laser vibrometer.

Experiment of laser vibrometer for the evaporator under ultrasonic excitation is shown in Fig. 14, the evaporator is fixed on the supporters by four binding screws which are fixed on the floor though a linker with the adjustable length. As shown in Fig. 14(b), the multiple mode frequencies of the evaporator are excited out at the moment when the ultrasonic transducer works. The maximum acceleration magnitude is found between the frequency of 28.4 kHz and 28.6 kHz, while the resonance frequency of the ultrasonic transducer is 28.2 kHz, there is a little difference between the resonance frequency and the working frequency. When the ultrasonic transducer is fixed on the evaporator, the impedance characteristic of the ultrasonic transducer is changed due to the presence of the evaporator which is imposed on the ultrasonic transducer as a load. The resonance frequency of ultrasonic transducer is drifted duo to the load, so the evaporator and the frost crystals are forced to vibrate at the ultrasonic transducer working frequency instead of the resonance frequency. The frost crystal fracture characteristics are coincidence with the resonance theory. One clear spectrum between 28.4 kHz and 28.6 kHz is shown in Fig. 14(c) after the transducer working stably, and the acceleration magnitude is larger than the maximum acceleration magnitude in Fig. 14(b) due to the energy concentrate on the resonance frequency of the ultrasonic transducer after it is working stable.

3.3.3. Analysis of ultrasonic defrosting mechanism

According to the basic principle of structural mechanics, the structure resonance which causes great dynamic response if the load frequency and the structure natural frequency is equal or close. When the evaporator is forced vibration under the excitation of ultrasonic vibration, the vibration frequency of frost crystals on the fin surface is equal to the vibration frequency of the evaporator. If the natural frequencies of the frost crystals are equal or match the frequency of evaporator vibration, the frost crystals will be resonance with high frequency and receive the most impact force, frost crystals removal from the cold surface can be achieved.

In the experiment, most of the frost crystals with certain shape and size are immediately broken up when the ultrasonic vibration is applied, the remaining frost crystals are gradually broken up with the frequency tracking of the ultrasonic power supply, the broken

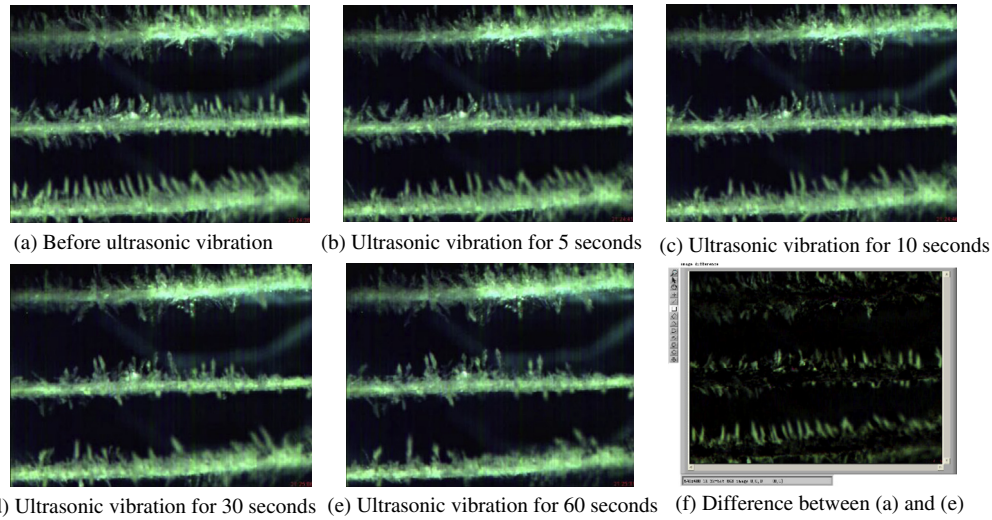

(a) Before ultrasonic vibration (b) Ultrasonic vibration for 5 seconds (c) Ultrasonic vibration for 10 seconds

(d) Ultrasonic vibration for 30 seconds (e) Ultrasonic vibration for 60 seconds (f) Difference between (a) and (e)

Fig. 13. The defrosting effect under ultrasonic high frequency vibration for 1 min.

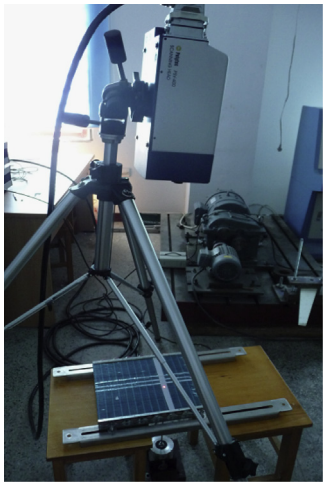

(a) Laser vibration measuring for the evaporator

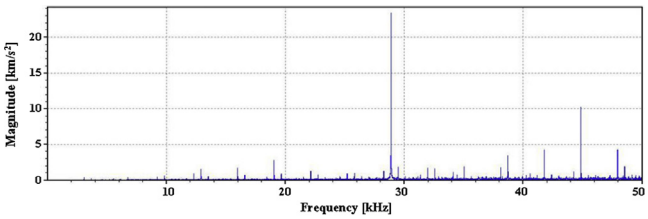

(b) Acceleration magnitude and frequency curve at ultrasonic excitation applied initially

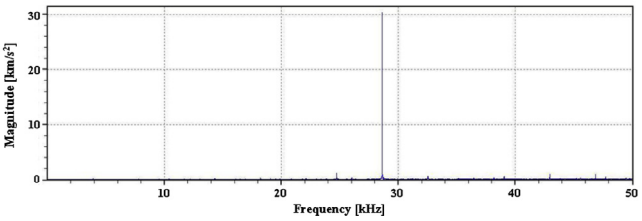

(c) Acceleration magnitude and frequency curve after ultrasonic excitation stabled

Fig. 14. Experimental of laser vibration measuring for the evaporator under ultrasonic excitation.

frost crystals fall off due to gravity. The laser vibrometer experiment showed that the evaporator is forced vibration at frequency of 28.2 kHz, therefore, the frost crystals on the fins surface are also forced vibration at frequency of 28.2 kHz. According to the frost crystal growth characteristics, the height of frost crystals are about 0.5 mm under the intermittent time of 4 min, numerical results show that the average natural frequency of 0.5 mm frost crystal under frost density $\rho_{min} = 50$ kg/m^3 and $\rho_{max} = 300$ kg/m^3 is about 27.9 kHz, which is similar to the forced vibration frequency of the evaporator. The results of the laser vibrometer experiment, the frost crystals breaking up characteristics, the frost crystals growing characteristics and the frost crystals frequency band distribution are coincide. The authors believe that the mechanism of ultrasonic defrosting is the resonance effect of natural frequency of frost crystals and excitation frequency, the amplitude is increased gradually and a strong stress is formed, which is the main reason of frost crystals suddenly broken up. Therefore, to realize high-efficiency and energy-saving defrosting for a finned-tube evaporator, the determination of optimal intermittent time should be based on the resonance frequency of the ultrasonic transducer, the frost crystal growth characteristic and the natural frequency distribution of frost crystal for the purpose of ultrasonic resonance defrosting.

3.3.4. Analysis of shear stress and acceleration effect

When ultrasonic is propagation in elastic medium, because the material physical parameters of frost and fin are different, the propagation velocity of ultrasonic is different in frost and fin. The shear stress is generated at the interface of frost layer and fin due to the velocity difference in two materials. The frost layer will detaching from the fin surface if the shear stress is larger than frost adhesion stress, which is the most desirable outcome. The double-layer system composed by frost layer and fin is shown in Fig. 15(a). The displacement field for ultrasonic in solid media is given by Eq. (1), which satisfy the Navier displacement motion equation [17].

$$\mu^n \nabla^2 u^n + (\lambda^n + u^n)\nabla(\nabla \cdot u^n) = \rho^n \frac{\partial^2 u^n}{\partial t^2} \tag{1}$$

The generalized displacement field is decomposing into two parts of dilatation wave and equivoluminal wave by using Helmholtz decomposition.

$$u^n = \nabla \phi^n + \nabla \times \psi^n \tag{2}$$

General solution of dilatation wave and equivoluminal wave for each layer is obtained by substitution boundary condition.

$$\begin{cases} \phi^n = C_1^n \exp\{ik_L^n[x_1 \sin(\theta_L^n) + x_3 \cos(\theta_L^n)]\} \\ \quad + C_2^n \exp\{ik_L^n[x_1 \sin(\theta_L^n) - x_3 \cos(\theta_L^n)]\} \\ \psi^n = C_3^n \exp\{ik_T^n[x_1 \sin(\theta_T^n) + x_3 \cos(\theta_T^n)]\} \\ \quad + C_4^n \exp\{ik_T^n[x_1 \sin(\theta_T^n) - x_3 \cos(\theta_T^n)]\} \end{cases} \tag{3}$$

In the case of having displacement field, substituting Eq. (3) into Eq. (2) based on strain–displacement relations and generalized Hooker's law, the stresses in the layered system are defined by Eq. (4).

$$\begin{cases} T_{zx}^n = \mu\left(\frac{\partial u_3^n}{\partial x_1^n} + \frac{\partial u_1^n}{\partial x_3^n}\right) = \rho\left(c_T^n\right)^2 \left(\frac{\partial^2 \psi^n}{\partial \left(x_3^n\right)^2} - \frac{\partial^2 \psi^n}{\partial \left(x_1^n\right)^2} + 2\frac{\partial^2 \phi^n}{\partial \left(x_3^n\right)^2 \partial \left(x_1^n\right)^2}\right) \\ T_{zy}^n = \mu\left(\frac{\partial u_3^n}{\partial x_2^n} + \frac{\partial u_2^n}{\partial x_3^n}\right) = \rho\left(c_T^n\right)^2 \left(\frac{\partial^2 \psi^n}{\partial (x_3^n)^2} - \frac{\partial^2 \psi^n}{\partial \left(x_2^n\right)^2} + 2\frac{\partial^2 \phi^n}{\partial (x_3^n)^2 \partial \left(x_2^n\right)^2}\right) \end{cases} \tag{4}$$

Fig. 15(b) shows the shear stress in *xy* plane, checking shear stress of each nodes on the icing area, comparing these shear stress value which is excited by ultrasonic to a typical adhesive shear strength value of glaze ice (0.4 MPa) [18], the stress of most nodes are larger than 0.4 MPa. Therefore, evaporator defrosting technology based on shear stress is feasible in theory. However, when the ultrasonic is normal incidence in frost layer and fin, a large amount of energy is reflected and transmitted, the energy remain on the frost layer and fin is litter, so the excited shear stress is not large enough for detach the frost layer from the fin surface, so the shear stress is not the main reason for evaporator defrosting.

According to the conclusion of laser vibrometer, evaporator and frost crystals on the fin surface are forced to vibrate under ultrasonic excitation frequency. In the case of having the torsion which is affected on the frost crystal, assuming the propagation of ultrasonic in the elastic medium is a standard cosine function without attenuation and damping. The displacement, velocity, acceleration and torsion are defined by Eq. (5).

$$\begin{cases} y = A * \cos(2 * pi * f_0 * t) \\ v = \dfrac{dy}{dt} = -A * (2 * pi * f_0) * \sin(2 * pi * f_0 * t) \\ a = \dfrac{dv}{dt} = A * (2 * pi * f_0)^2 * \cos(2 * pi * f_0 * t) \\ T = F * L = m * a * L = m * A * (2 * pi * f_0)^2 * \cos(2 * pi * f_0 * t) * L \end{cases} \tag{5}$$

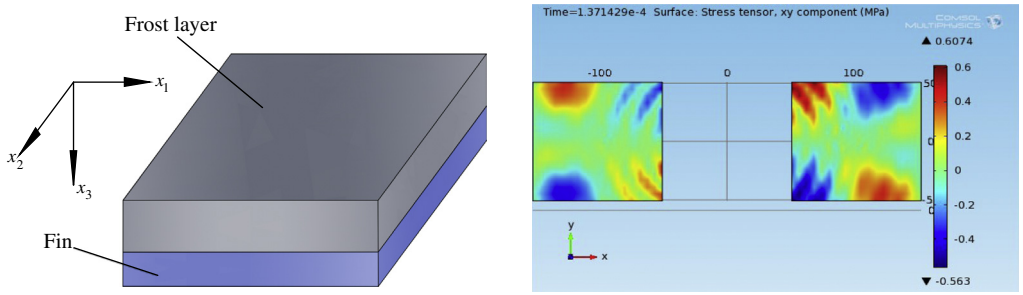

(a) guided wave propagation in double-layer structure

(b) Shear stress in x_1x_2 plane under 28.2 kHz

Fig. 15. Schematic of guided wave propagation and shear stress excitation in double-layer structure.

Compared with the low-frequency vibration, the frost crystals are withstand great torque under ultrasonic high frequency vibration, and peak acceleration excited by ultrasonic frequency of 28 kHz is 23.39 km/m^2, which is 2339 times of the gravity acceleration. In a short time, the frost crystals are fatigue and break up in root due to the great torque produced by acceleration, if the natural frequency of frost crystals and frequency of ultrasonic vibration are similar or same, this phenomenon is more pronounce, that is the reason why low frequency vibration was not defrosting effective.

4. Conclusions

The main ultrasonic defrosting mechanism is resonance effect which is based on theoretical analysis and experimental study, form the experimental investigation, the conclusions can be drawn as follows:

(1) Natural frost experiment shows that the height of the frost crystals is about 0.5 mm after growing for 4 min, and the natural frequency is near to the working frequency of ultrasonic transducer according to the numerical calculation. Therefore, it is possible that the early frost crystals and the ultrasonic vibration excitation have resonance characteristic.
(2) The frost crystals of similar in shape and size are falling off instantly when the ultrasonic transducer works, the results of laser vibrometer show that the evaporator and the frost crystals on the fin surface are forced to vibrate at the working frequency of the ultrasonic transducer. Therefore, the frost crystals and the ultrasonic transducer have resonance characteristics.
(3) The intervention of ultrasonic vibration at the initial frosting stage prevent frost crystals crossed growth, so the intermittent time should be controlled within 6 min, the optimal working mode recommended in this paper is intermittent 4 min, vibration 1 min based on the intermittent ultrasonic resonance defrosting experiment.
(4) The main mechanism of ultrasonic defrosting is the resonance effect of natural frequency of frost crystals and excitation frequency. Shear stress produced by velocity difference at the interface of frost layer and fin is larger than 0.4 MPa. Therefore, the defrosting technology based on shear stress is feasible in theory, and more practical application need further study. A great torque which excited by ultrasonic vibration impel frost crystals fatigue or break up in a short time. In conclusion, the mechanism of ultrasonic defrosting is the combination effect of ultrasonic resonance characteristic, ultrasonic shear stress and acceleration effect of ultrasonic.

Acknowledgment

The authors would wish to thank Key Science and Technology Program of Shaanxi Province (2012k09-16) for offering the funds to the studied.

References

[1] Z. Liu, G. Tang, F. Zhao, Dynamic simulation of air-source heat pump during hot-gas defrost, Applied Thermal Engineering 23 (2003) 675–685.
[2] H. Cho, Y. Kim, I. Jang, Performance of a showcase refrigeration system with multi-evaporator during on-off cycling and hot-gas bypass defrost, Energy 30 (2005) 1915–1930.
[3] N. Hoffenbecker, S.A. Klein, D.T. Reindl, Hot gas defrost model development and validation, International Journal of Refrigeration 28 (2005) 605–615.
[4] M. Qu, S. Deng, Y. Jiang, An experimental study on the defrosting performance of a PCM-based reverse-cycle defrosting method for air source heat pumps, International Journal of Air-Conditioning and Refrigeration 4 (2010) 327–337.
[5] J. Alberto Dopazo, J. Fernandez-Seara, F.J. Uhia, R. Diz, Modeling and experimental validation of the hot-gas defrost process of an air-cooled evaporator, International Journal of Refrigeration 33 (2010) 829–839.
[6] T. Munakata, A. Yabe, I. Tanasawa, Effect of Electric Fields on Frosting Phenomenon, International Journal of Fluid Mechanics Research 25 (1998) 588–599.
[7] C. Wang, R. Huang, W. Sheu, Y. Chang, Some observations of the frost formation in free convection: with and without the presence of electric field, International Journal of Heat and Mass Transfer 47 (2004) 3491–3505.
[8] V. Tudor, M. Ohadi, The effect of stationary and sweeping frequency AC electric fields on frost crystal removal on a cold plate, International Journal of Refrigeration 29 (2006) 669–677.
[9] X. Zhang, Z. Liu, J. Wang, Y. Gou, S. Meng, S. Cheng, Influence of surface characteristics on frost formation on vertical cold plate with electric field, Journal of Refrigeration 27 (3) (2006) 54–58 (in Chinese).
[10] C.M. Joppolo, L. Molinaroli, S.D. Antonellis, U. Merlo, Experimental analysis of frost formation with the presence of an electric field on fin and tube evaporator, International Journal of Refrigeration 35 (2012) 468–474.
[11] K. Adachi, K. Saiki, H. Sato, Suppression of frosting on a metal surface using ultrasonic vibrations, in: IEEE Ultrasonic Symposium, 1998, pp. 759–762.
[12] K. Adachi, K. Saiki, H. Sato, T. Ito, Ultrasonic frost suppression, Japan Journal of Applied Physics, Part 1-Regular Papers Short Notes Review Papers 42 (2003) 682–685.
[13] Q. Yan, L. Zhu, N. Yan, Study on ultrasonic defrost technology of refrigeration fan, Journal of Agriculture and Machine 34 (2003) 74–75 (in Chinese).
[14] D. Li, Z. Chen, M. Shi, Effect of ultrasound on frost formation on a cold flat surface in atmospheric air flow, Experimental Thermal and Fluid Science 34 (8) (2010) 1247–1252.
[15] D. Wang, T. Tao, G. Xu, A. Luo, S. Kang, Experimental study on frosting suppression for a finned-tube evaporator using ultrasonic vibration, Experimental Thermal and Fluid Science 36 (2012) 1–11.
[16] Y. Yao, Y. Jiang, Z. Ma, Change of frost density and thickness for finned-tube heat exchanger under frosting, Journal of Engineering Thermophysics 24 (6) (2003) 1040–1042 (in Chinese).
[17] J.L. Rose, Ultrasonic waves in solid media, in: He Cunfu, Wu Bin, Wang Xiuyan (Eds.), Translation, Beijing Science Press, 2004, pp. 143–157 (in Chinese).
[18] M.C. Chu, R.J. Scavuzzo, Adhesive shear strength of impact ice, AIAA Journal 29 (11) (1991) 1921–1926.